0^+ states in deformed actinide nuclei by the (p,t) reaction

H.-F. Wirth,[1] G. Graw,[1] S. Christen,[2] D. Cutoiu,[3] Y. Eisermann,[1] C. Günther,[4] R. Hertenberger,[1] J. Jolie,[2] A. I. Levon,[5] O. Möller,[2] G. Thiamova,[6] P. Thirolf,[1] D. Tonev,[2] and N. V. Zamfir[7]

[1]*Sektion Physik, Ludwig-Maximilians-Universität München, D-85748 Garching, Germany*

[2]*Institut für Kernphysik, Universität zu Köln, D-50937 Köln, Germany*

[3]*Horia Hulubei Institute of Physics and Nuclear Engineering, 76900 Bucharest, Romania*

[4]*Helmholtz-Institut für Strahlen- und Kernphysik, Universität Bonn, D-53115 Bonn, Germany*

[5]*Institute for Nuclear Research, Academy of Science, 03680 Kiev, Ukraine*

[6]*Nuclear Physics Institute, 25068 Řež, Czech Republic*

[7]*Wright Nuclear Structure Laboratory, Yale University, New Haven, Connecticut 06520, USA*

(Received 7 October 2003; published 16 April 2004)

By means of the (p,t) reaction we study the excitation spectra of 0^+ states in the deformed nuclei ^{228}Th, ^{230}Th, and ^{232}U, using the Q3D magnetic spectrograph facility at the Munich tandem accelerator. At small reaction angles the 0^+ transfer angular distributions have steeply rising cross sections which allow us to identify these states in otherwise very complicated and dense spectra. For each of these nuclei we resolve typically about ten excited states with safe 0^+ assignments. The studied excitation energies range up to 2.5, 2.7, and 2.3 MeV, respectively, and the summed transfer strengths add to more than 60% of the ground state strength. As in a recent study of ^{158}Gd we compare with interacting boson approximation (IBA) calculations in the *spdf* boson space. This highly schematic collective model description, including octupole collectivity, but neglecting other relevant degrees of freedom, gives numbers of excited 0^+ states in these actinide nuclei that are rather close to the observed ones.

DOI: 10.1103/PhysRevC.69.044310 PACS number(s): 21.10.Jx, 21.60.Ev, 27.90.+b

I. INTRODUCTION

In nuclei the appearance of excited 0^+ states is indicative for the presence of specific modes of nuclear excitations, and their study is therefore of considerable interest. For the closed shell nucleus ^{208}Pb only two excited 0^+ states have been observed so far: a neutron pairing vibrational mode [1] and an octupole two-phonon excitation [2–4]. Intruder configurations may contribute in addition as known for ^{40}Ca and for less closed nuclei as ^{90}Zr, ^{96}Zr [5], ^{112}Cd [6], and others. In deformed nuclei a large variety of excited 0^+ states is expected as discussed in detail below.

Excited 0^+ states are easily identified via (p,t) and (t,p) reactions in otherwise complicated and dense excitation spectra, because they have steeply rising cross sections at small reaction angles; at the same time only natural parity states are populated strongly. Rich 0^+ spectra had been observed in earlier (p,t) studies of medium weight nuclei as ^{146}Nd [7], ^{146}Sm [8], ^{134}Ba, ^{132}Ba [9], and ^{114}Sm [10], where typically nine excited 0^+ states had been resolved in the excitation energy range up to 2.5–4 MeV. To reproduce theoretically the number of 0^+ states in ^{146}Nd and ^{146}Sm and to account for the excitation strengths in (p,t), specific particle-hole and particle-particle correlations had to be considered in addition to particle-core coupling effects [7,8].

In addition to 0^+ transfer from $J^\pi=0^+$ target nuclei one has to mention 0^+ transfer studies in (p,t) from target nuclei with spin, e.g., the study of the ground state and of related higher states in ^{229}Pa [11], and the study of the distribution of $7/2^-$ strength in odd samarium isotopes by Trache *et al.* [12]. In deformed heavy nuclei the low-lying 0^+ states had been studied systematically in the early 1970s.

For rare earth nuclei Oothoudt and Hintz [13] observed in (p,t) typically three excited 0^+ states. The cross sections for the ground states are about the same, while for the excited states they differ significantly: For many nuclei the first excited 0^+ states have low cross sections, a few percent compared to the ground state, and the next higher states are typically a bit stronger. On the other hand, nuclei as ^{174}Yb (and ^{176}Hf) have for the first excited 0^+ states the large cross sections of 25% (and 12%) of the ground state excitation.

For the actinides Maher *et al.* [14] observed in (p,t) also strong excitations of the first excited 0^+ states. Combined with other available evidence, in particular, the strong Coulomb excitation of the associated rotational bands, they concluded that these 0^+ states represent a stable collective excitation different in character from both the β vibration and the most common formulation of the pair vibration.

To explain these observations, Griffin, Jackson, and Volkov [15], van Rij and Kahana [16], and Bess, Broglia, and Nilsson [17] realized the importance of the quadrupole pairing field—in addition to the monopole pairing—for deformed nuclei. In combination with a nonstochastic distribution of oblate and prolate single particle orbitals these strongly excited low-lying 0^+ states result as pairing isomer states. Consistent with this model was the nonobservation of these states in (t,p) in a search on actinide nuclei by Casten *et al.* [18]. These studies culminated in the microscopic calculations of low-lying 0^+ states in actinides by Ragnarsson and Broglia [19]. A later study of the W isotopes by Mortensen, Betts, and Bockelmann [20] revealed also the importance of excitations associated with a subshell gap, in addition to the pairing isomer mechanism.

In recent years a few more 0^+ states had been identified [21–24], but the understanding of the higher excited 0^+ states

remains as a challenge for nuclear theory. Within their quasiparticle model (QPM) Soloviev and co-workers [25–28] provided microscopic understanding of low-lying 0^+ states. We have to refer also to the study of Otsuka and Sugita [29] which deals with the *spdf*-IBM (interacting boson model) in application to the actinide nuclei. These calculations were restricted to the first two 0^+ excitations (known to this time).

A renewed interest in 0^+ states results from a recent (p,t) study of ^{158}Gd of Lesher *et al.* [30], where 13 excited 0^+ states have been identified at excitation energies below 3.1 MeV, with an accumulated transfer strength of about 25% of the ground state strength. Note that, as for some of the W-Pt nuclei [14], the (p,t) transfer strength to the first excited 0^+ state of ^{158}Gd is weak.

In the present paper we report on a study of 0^+ states in the actinide nuclei ^{228}Th, ^{230}Th, and ^{232}U, observed in (p,t) spectra. The choice of the nuclei was restricted by the availability of the respective targets. Our experimental results about states with J^π values different from 0^+ or of weakly excited states, where tentative 0^+ assignments may be possible, will be presented in separate publications [31].

We obtain new and detailed experimental information about the 0^+ excitation spectra and their strength distributions in (p,t). For each of these three nuclei the accumulated transfer strengths add up to about 60% of the ground state strengths. This value is much larger than observed for lighter nuclei and it will be interesting to understand this feature.

The neutron pairing gap parameter for these nuclei is in the vicinity of 700 keV, which leads to two-quasiparticle excitations around 1.5 MeV. One thus expects a remarkable number of 0^+ states above this energy, as predicted in the calculations of Ragnarsson and Broglia [19] mentioned above.

To obtain an estimate for the number of excited 0^+ states which result from quadrupolar and octupolar collectivity, we also discuss respective interacting boson approximation (IBA) calculations, which support the relevance of octupole collectivity. In this model in lowest order the respective transfer strengths vanish for the higher excited states. Introducing higher order terms this is corrected to some extent, but this will not be presented here. This restricts the comparison with the experimental data, also because we may miss experimentally some 0^+ states with very low transfer strength.

The large cross sections of the many observed 0^+ states in ^{228}Th, ^{230}Th, and ^{232}U, and the respective (p,t) transfer strength distributions provide a test case for modern microscopic structure calculations, which include the various aspects of interaction and collectivity.

II. EXCITED 0^+ STATES IN DEFORMED NUCLEI

The present calculations of 0^+ excitation energies and (p,t) strengths in deformed heavy nuclei are restricted to the low energy range. For the more extended energy range that we have to consider, a number of structure effects are expected to contribute. In comparison to spherical nuclei additional 0^+ states have to be expected in deformed nuclei because of the quantization with respect to the intrinsic axis:

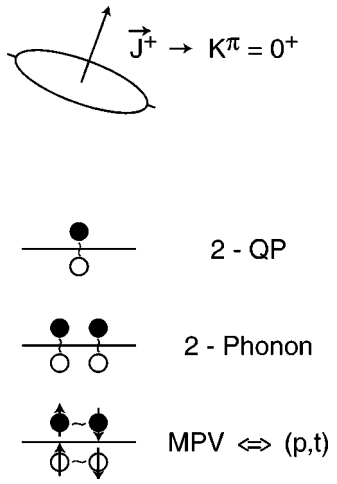

FIG. 1. Schematic presentation of the different kinds of excitations in deformed nuclei, yielding excited $K^\pi=0^+$ states: Positive parity two-quasiparticle excitations (of collective and of noncollective nature), two-phonon excitations, and monopole pairing excitations.

An excitation mode with angular momentum J^π splits into states distinguished by their K quantum numbers, which range from zero to J, compare Fig. 1. Thus, e.g., a quadrupolar (one-phonon) vibration with $J^\pi=2^+$ splits into $K^\pi=0^+$ and $K^\pi=2^+$ states, an example is the heads of the related β and γ vibrational bands.

For axially symmetric deformed nuclei 0^+ states result from K splitting of collective and of noncollective modes of excitation. For most quantum numbers of natural parity the lowest states are collective, compare, e.g., ^{208}Pb [4]. States related to specific two-quasiparticle modes are expected to follow at higher excitation energies above twice the pairing gap energy, around 1.5 MeV in our case. In addition, there are the two-phonon excitations of the collective modes at low energies, the quadrupole, octupole and hexadecupole phonons. Apart from these we have to consider the collective monopole pairing vibration (MPV). In reality all these configurations will mix to some extent. In (p,t) the observed spreading of the excitation strength of the higher lying excited 0^+ states may be treated as mixing with the neutron component of the MPV.

A. Quadrupole and octupole collectivity

Accounting for quadrupole and octupole collectivity only, in Ref. [32] the IBA was used within the *spdf* boson space to see how many of the excited 0^+ states are expected for ^{158}Gd in this energy range, and to compare this with the 13 excited 0^+ states identified by Lesher *et al.* [30]. The calculations of Ref. [32] had been restricted to a highly schematic discussion: the simplest form of the Hamiltonian is used and mixing between *d* and *pf* bosons is neglected. The parameters are chosen to reproduce the excitation energies of low-lying spectra, especially the bands of negative parity. In the energy range considered, their IBA calculation predicts five excited 0^+ states of pure *sd* (quadrupolar) bosonic structure—as in the geometrical collective model—and three additional ex-

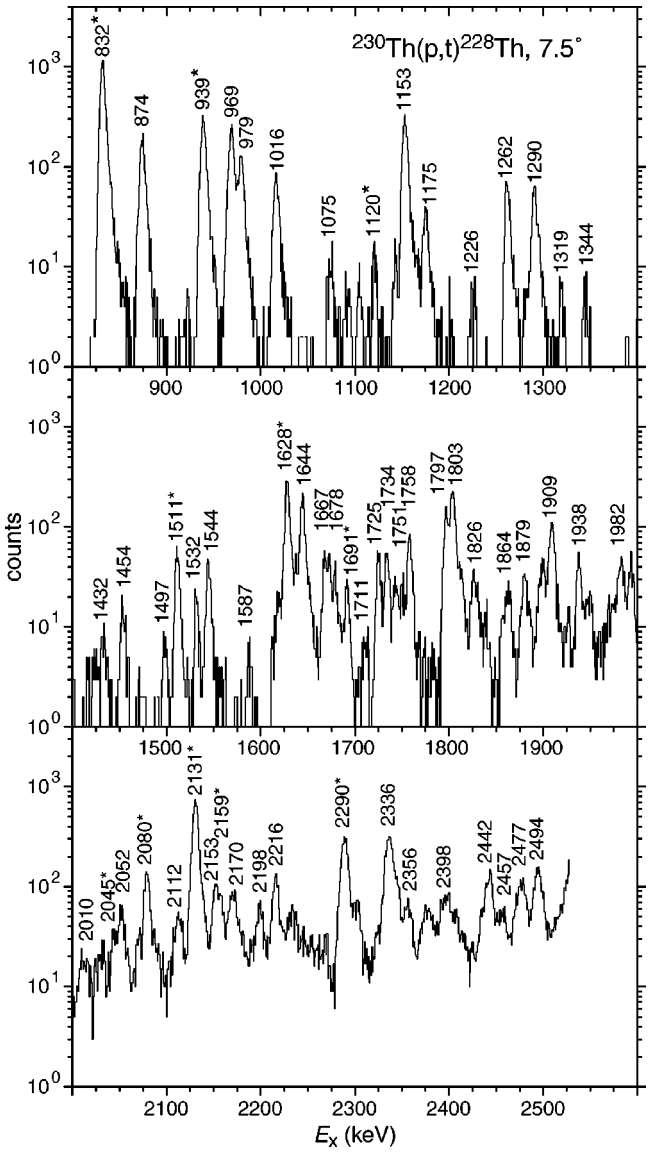

FIG. 2. Spectrum for the ^{230}Th$(p,t)^{238}$Th reaction (E_p =25 MeV) at a detection angle of 7.5° in logarithmic scale, in the energy range beginning with the first excited 0^+ state. Some levels are labeled with their excitation energy in keV. States assigned as 0^+ are marked with an asterisk.

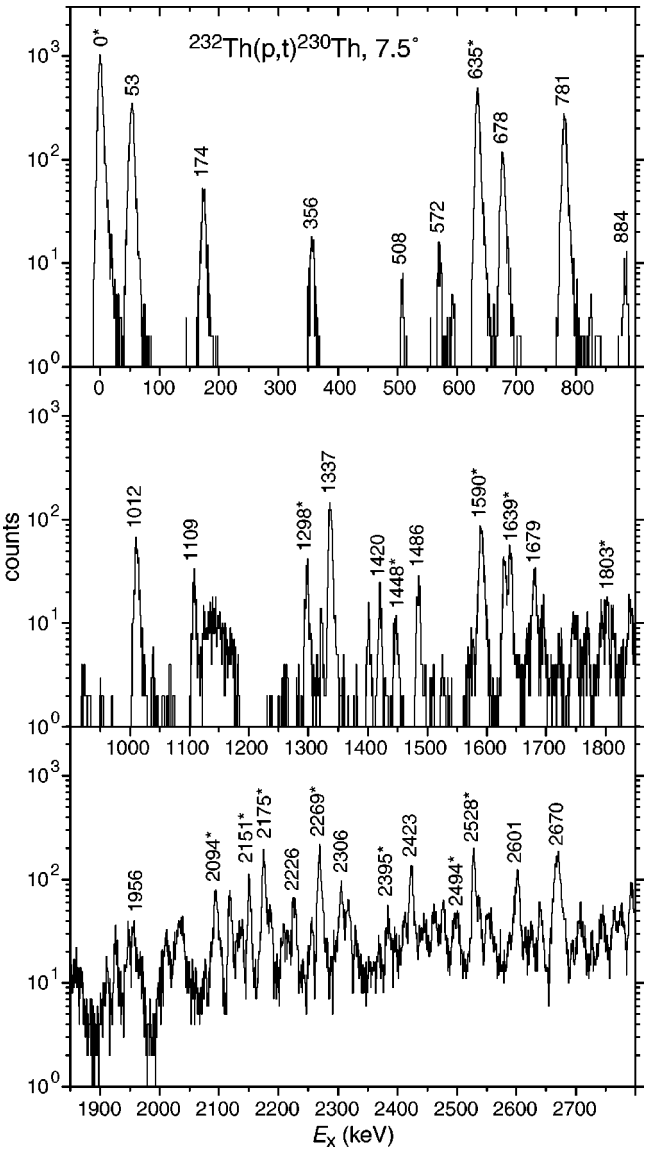

FIG. 3. Complete spectrum for ^{232}Th$(p,t)^{230}$Th (E_p=25 MeV) in logarithmic scale for a detection angle of 7.5°. Some levels are labeled with their excitation energy in keV. States assigned as 0^+ are marked with an asterisk.

cited 0^+ states with two bosons in the *pf* boson space. The latter ones are related to octupole two-phonon (OTP) excitations. The model provides some kind of educated guess about the number of excited 0^+ states resulting from quadrupolar and octupolar collectivity.

In the present study of actinide nuclei we deal with deformed nuclei of strong octupole collectivity, which, however, changes with the mass number. A measure of the octupole collectivity is given by the excitation energy of the first 1^- state. Compared to ^{158}Gd with $E_x(1^-)=977$ keV the excitation energies of ^{228}Th, ^{230}Th, and ^{232}U are $E_x(1^-)=328$, 508, and 563 keV, respectively. Thus, we are in a position to compare three neighboring nuclei which differ by one neutron pair and/or by one proton pair only but vary strongly with respect to octupole collectivity. The experimental information about the low-lying states of ^{228,230}Th and ^{232}U is summarized in Refs. [33–35] and several more recent experimental investigations [21–24,28,36,37], including a (p,t) study of the lowest states [23]. Addressed to theoretical understanding of these nuclei there are a number of recent publications which are related mainly to features of octupole collectivity [38–44], triaxiality [45,46], and to the description within interacting boson approximations [47–52].

In axially symmetric, statically deformed nuclei any excitation of positive parity causes a $K^\pi=0^+$ state. Since the nuclei we study are prolate we have to expect, as for Nilsson states, strongest binding for the lowest K state. This enhances the number of 0^+ states at low excitation energies. Large energy shifts result from the K splitting of the octupole vibrational state, as discussed by Cottle and Zamfir [47] in the case of rare earth nuclei: the $K^\pi=0^-$ and $K^\pi=1^-$ bandheads

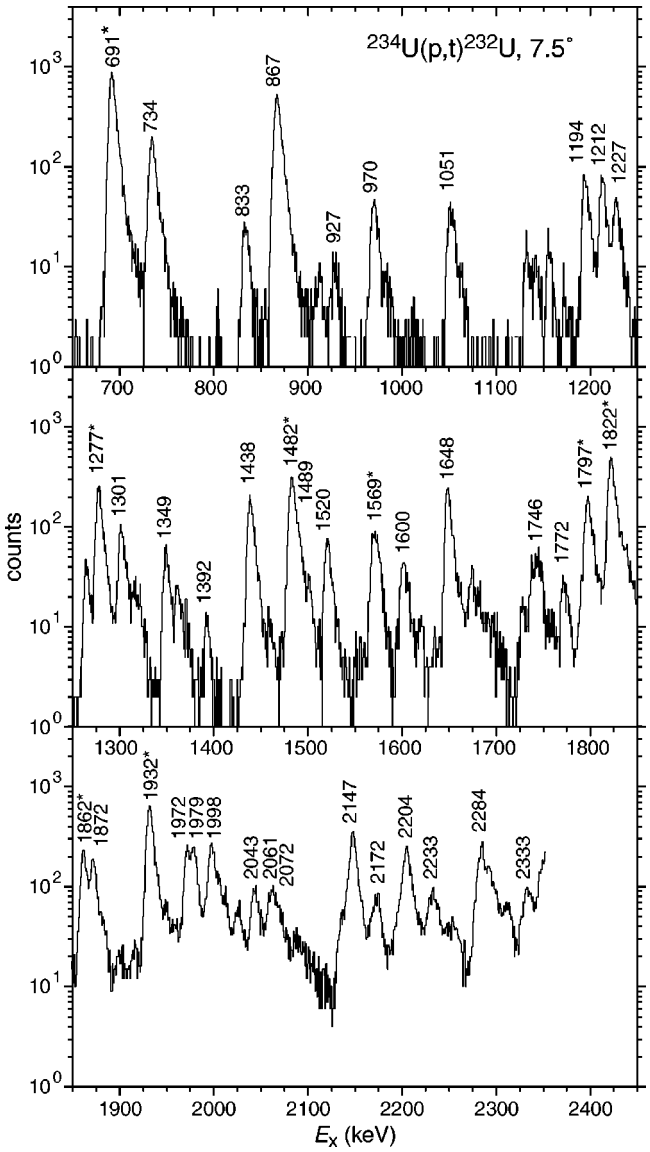

FIG. 4. Spectrum for ^{234}U$(p,t)^{232}$U(E_p=25 MeV) in logarithmic scale for a detection angle of 7.5°, in the energy range beginning with the first excited 0^+ state. Some levels are labeled with their excitation energy in keV. States assigned as 0^+ are marked with an asterisk.

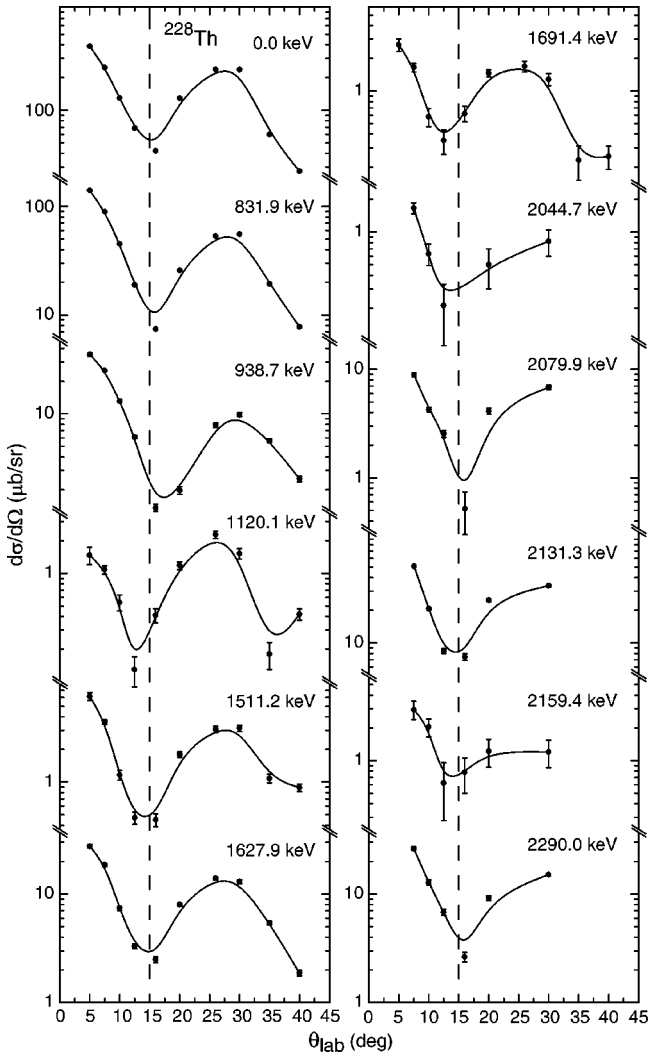

FIG. 5. Angular distributions of assigned 0^+ states in ^{228}Th. The lines are drawn to guide the eyes and have no further meaning.

are observed at very low excitation energies, whereas the $K^\pi=3^-$ strength is shifted upwards in energy.

In the IBA study of 0^+ states in ^{158}Gd [32] the octupolar excitations contribute to the number of $K^\pi=0^+$ states via two-phonon excitations only. Since the coupling of these two-phonon octupole excitations with quadrupole phonon excitations is neglected, the *sdf*-IBA calculation gives the $K^\pi=0^+$ excitations of pure quadrupolar type at exactly the same energies as a pure *sd*-IBA, and all additionally calculated $K^\pi=0^+$ states result with a pure f^2 boson content, equivalent to octupole two-phonon excitations.

B. Further degrees of freedom

Collective excitations of multipolarity 0^+ and 4^+, the MPV excitation, and some hexadecupole vibrational collectivity, have to be expected and shall lead to a number of additional excited $K^\pi=0^+$ states.

The monopole pairing vibration is well established for ^{208}Pb. Of the two known 0^+ states of ^{208}Pb, the lower one is identified as the MPV state and the higher one as the 0^+ member of the octupole-two-phonon excitation multiplet, compare Ref. [4] and further references therein. According to the literature one expects at least two kinds of MPV states, one for neutron-pair excitations (*n*-MPV) and one for proton-pair excitations (*p*-MPV). The latter one usually is expected at higher excitation energy. Because of its collective (vibrational) nature, in a (p,t) reaction the *n*-MPV state is expected to be strongly excited. In case of a relatively dense spectrum of 0^+ states the *n*-MPV state will mix with nearby states. In our case mixing is significant and we may consider the center of the transfer strength—at an excitation energy near 1600 keV (see Fig. 11)—as the unperturbed excitation energy of the neutron monopole pairing vibration (*n*-MPV) state. The pairing vibrational excitations result from a particle-particle coupling in the residual interaction, which, however, is not included in the usual RPA- or IBA-like struc-

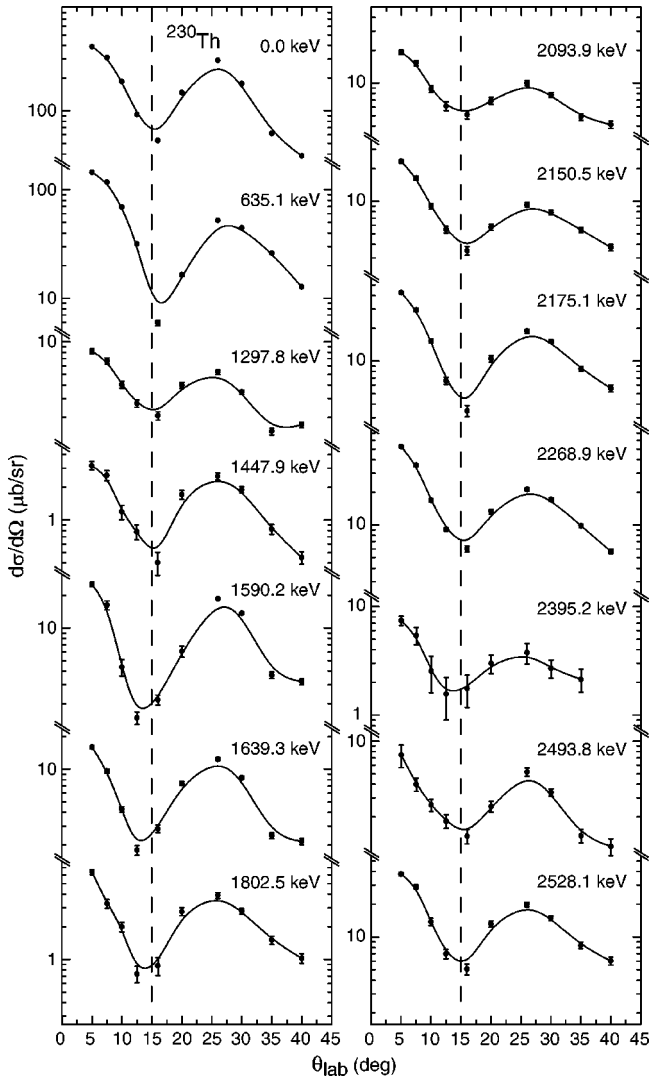

FIG. 6. Angular distributions of assigned 0^+ states in ^{230}Th. The lines are drawn to guide the eyes and have no further meaning.

ture calculations. Within these frames the pairing vibrational excitation has to be considered as a kind of intruder configuration.

Hexadecupole vibrational collectivity is established in spherical nuclei at excitation energies near or slightly above the collective octupole state. In inelastic scattering it is related with large one-step transition strength to excited 4^+ states. The analysis of hexadecupole collectivity is complicated because of the necessity to differentiate against quadrupole two-phonon 4^+ excitations and related processes. Also the hexadecupole strength may be distributed over a few neighboring states, in contrast to the octupole strength, which is concentrated in the lowest 3^- state. One may compare with a study of ^{112}Cd by Hertenberger *et al.* [6] and Garrett *et al.* [53]. As for the octupole vibration, it is reasonable to assume that the $K^\pi=0^+$ hexadecupole excitation will be pushed down to rather low energy. This may be treated formally by introducing a *g* boson and expanding a *sd*-IBA to a *sdg*-IBA, analogous to the case of octupole collectivity. In this way additional $K^\pi=0^+$ states shall be derived.

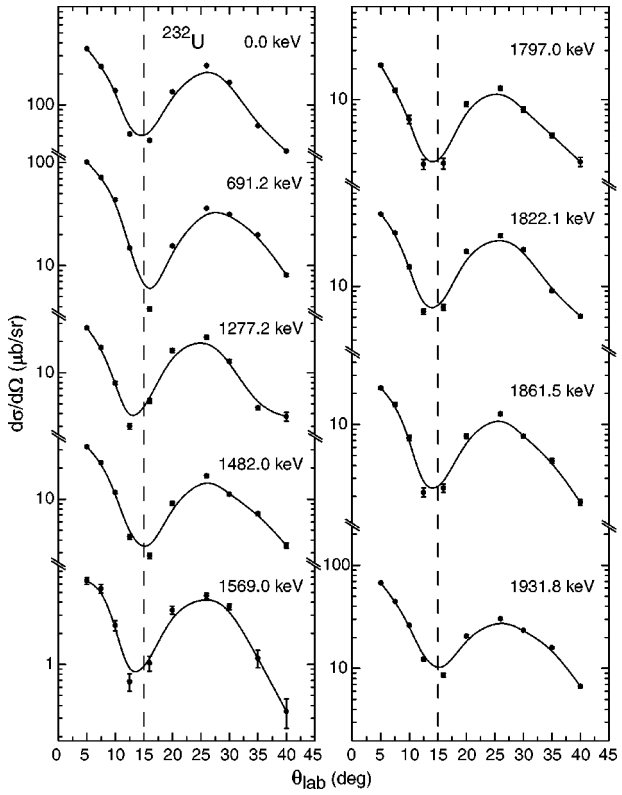

FIG. 7. Angular distribution of assigned 0^+ states in ^{232}U. The lines are drawn to guide the eyes and have no further meaning.

The very interesting question with respect to the observed (p,t) strength is the contribution of noncollective $K^\pi=0^+$ states, resulting from noncollective two-quasiparticle (2QP) excitations. It is the concept of collectivity that for each given multipolarity J^π the noncollective 2QP excitations are expected at considerable higher energy than the respective collective vibrational states. It will be very interesting to see microscopic calculations extending the study of Ragnarsson and Broglia [19] to higher energies, to learn about the nature of the observed states.

III. EXPERIMENTS

A. Experimental procedure, spectra

The (p,t) experiments have been performed at the Munich tandem accelerator laboratory with a beam of 25 MeV protons and intensities of $1-2$ μA on target. The reaction products have been analyzed with the Q3D magnetic spectrograph [54] and detected in its focal plane. We used two different focal plane detectors which are multiwire proportional chambers with readout of a cathode foil structure for position determination and $\Delta E/E_{\rm rest}$ particle identification [55–57]. The targets ^{230}Th, ^{232}Th, and ^{234}U had a thickness of 100 μg/cm^2 each, evaporated onto 22 μg/cm^2 thick carbon backings. The isotopic purity of the ^{230}Th and ^{234}U targets was about 99%. The resulting triton spectra have a resolution of $5-7$ keV full width at half maximum and are virtually background-free. Angular distributions of the cross sections are extracted from spectra at ten different laboratory

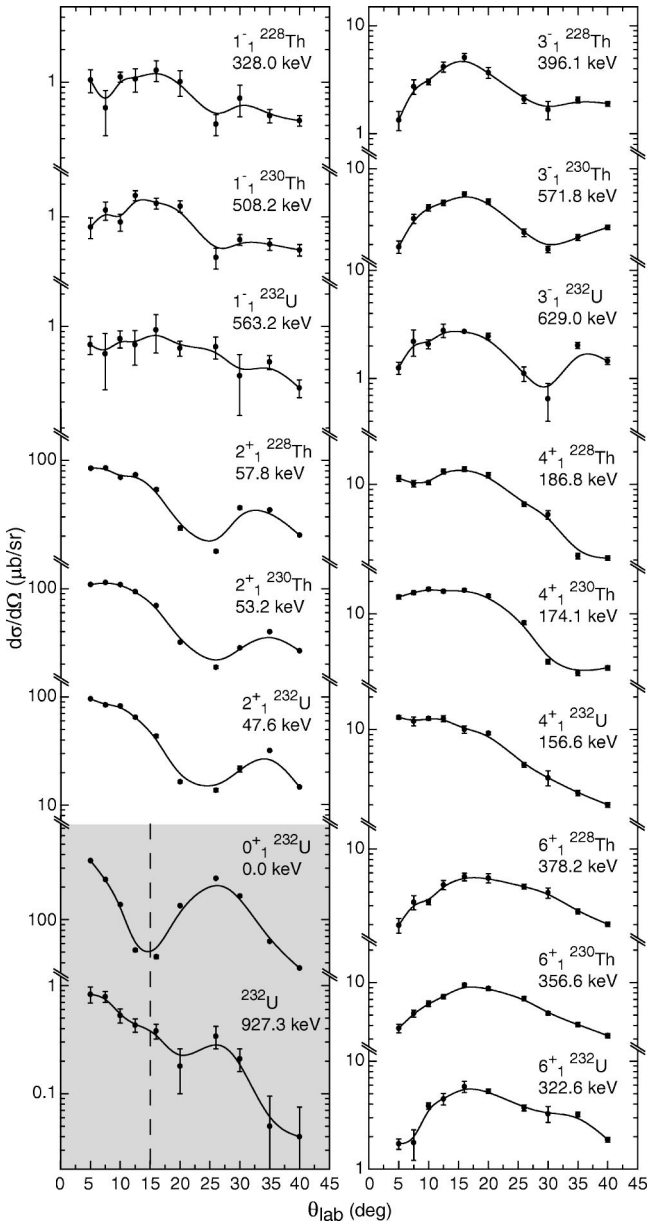

FIG. 8. Angular distributions of the first excited 1^-, 2^+, 3^-, 4^+, and 6^+ states. In the shaded area we compare the angular distributions of the ^{232}U 0^+ ground state and the 927.3 keV excited state. This angular distribution does not allow for a firm 0^+ assignment proposed by Ardisson *et al.* [59]. The lines are drawn to guide the eyes and have no further meaning.

angles (5°, 7.5°, 10°, 12.5°, 16°, 20°, 26°, 30°, 35°, 40°).

In the case of ^{230}Th$(p,t)^{228}$Th we have at higher excitation energies spectra for five angles only (7.5°, 12.5°, 16°, 20°, 30°) because of problems with the target.

Typical spectra for a detection angle of 7.5° are shown in Figs. 2–4 for the three nuclei. At this angle the 0^+ states have comparatively large cross sections. For calibration purposes spectra from different target nuclei had been taken in the same magnetic setting, including the reactions ^{184}W(p,t) and ^{186}W(p,t). The triton spectra were analyzed with the program GASPAN of Rieß [58].

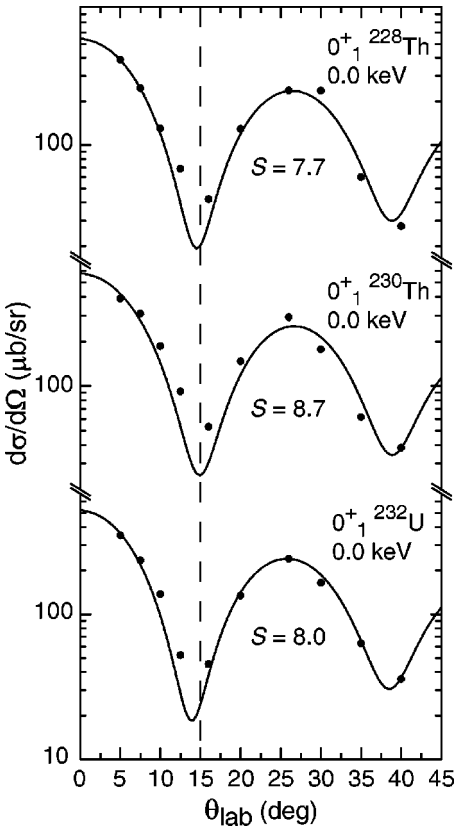

FIG. 9. Ground state transition data with DWBA fits. The spectroscopic factors $S=(d\sigma/d\Omega)^{\mathrm{expt}}/(d\sigma/d\Omega)^{\mathrm{CHUCK3}}$ are given.

B. Experimentally obtained 0^+ states

The 0^+ transfers are identified from their typical pattern in the differential cross section angular distributions. At very small reaction angles the 0^+ transfer angular distributions

TABLE I. Optical potential parameters used in the DWBA calculations. The values were chosen according to Ref. [61].

		(p,t)Th,U			$(p,t)^{158}$Gd		
E_p	(MeV)	25			27		
		p	t	n	p	t	n
V_r	(MeV)	57.10	166.70	[a]	58.88	160.03	[a]
$4W_D$	(MeV)	32.46			29.80		
W_0	(MeV)	2.80	10.28		3.24	17.83	
$4V_{so}$	(MeV)	24.80		$\lambda=25$	24.80		$\lambda=25$
r_r	(fm)	1.17	1.16	1.17	1.23	1.20	1.17
r_D	(fm)	1.32			1.32		
r_0	(fm)	1.32	1.50		1.32	1.40	
r_{so}	(fm)	1.01			1.01		
R_c	(fm)	1.30	1.30		1.25	1.30	
a_r	(fm)	0.75	0.75	0.75	0.75	0.72	0.75
a_D	(fm)	0.51			0.65		
a_0	(fm)	0.51	0.82		0.65	0.84	
a_{so}	(fm)	0.75			0.75		
nlc		0.85	0.25		0.85	0.25	

[a]Adjusted by CHUCK3.

have steeply rising cross sections and a sharp minimum at a detection angle of ≈15°. This allows us to identify these states in otherwise very complicated and dense spectra.

The differential cross section angular distributions of those observed transfers to ^{228}Th, ^{230}Th, and ^{232}U, which we assign as 0^+ are shown—in logarithmic scale—in Figs. 5–7. These are all angular distributions which are very similar in shape to the respective ground state transitions. Since all these distributions are rather similar we use lines to guide the eye.

One may compare these angular distributions with those for transitions with different quantum numbers: Fig. 8 shows angular distributions of transitions to the first excited 1^-, 2^+, 3^-, 4^+, and 6^+ states of these nuclei in comparison to the 0_1^+ state of ^{232}U. The 1^- transitions are very weak and may result from multistep excitations. All the other rather strong transitions show J^π typical shapes: The angular position of the first minimum in cross section shifts systematically with increasing transferred angular momentum. For a given quantum number the distributions for ^{228}Th, ^{230}Th, and ^{232}U are very similar.

Since we have no knowledge of the microscopic structure of these levels, the assignments of quantum numbers at present is restricted to this kind of pattern recognition. In (p,t) for a given quantum number J^π we can expect—at least in the limit of DWBA (distorted-wave Born approximation)—relative cross section angular distributions rather independent of the specific structure of the individual state, since the wave function of the outgoing triton is restricted to the nuclear exterior, and thus to the tails of the transition form factors.

In the shaded area of Fig. 8 we compare the angular distributions of the 927 keV excited state in ^{232}U with the 0^+ ground state. The angular distribution of the 927 keV state gives no firm evidence for a 0^+ assignment proposed by Ardisson *et al.* [59].

C. DWBA analysis and transfer strengths

Assuming transfer of a given (lj) pair, coupled to spin zero, DWBA calculations give cross section angular distribu-

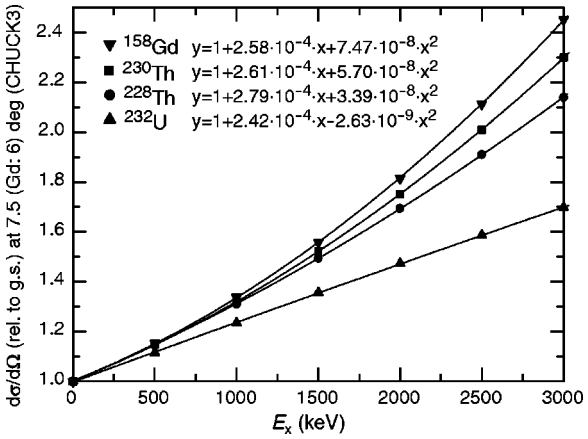

FIG. 10. DWBA calculations of cross sections of excited 0^+ states at 7.5° normalized to the ground state cross section (calculated with CHUCK3 using the input files of Fig. 15).

TABLE II. Assigned 0^+ states in ^{228}Th, ^{230}Th, and ^{232}U. The transfer strength of the excited states adds up to 64, 64, and 72% of the observed ground state strength, respectively.

E_x (keV) This work	E_x (keV) NDS [33–35]	$\sigma(\theta=7.5°)$[a] (μb/sr)	Spectroscopic factor (%)
	^{228}Th		
0.0	0.0	246.6	100.0[b]
831.9(3)	831.823(10)	89.4	28.9
938.7(3)	938.58(7)	25.0	7.8
1120.1(3)	1120.09(10)[c]	1.1	0.3
1511.2(3)		3.6	1.0
1627.9(3)		18.6	4.9
1691.4(4)		1.7	0.4
2044.7(5)		1.7	0.4
2079.9(5)		8.9	2.1
2131.3(6)		50.7	11.8
2159.4(5)		3.0	0.7
2290.0(7)		26.3	5.9
Σ			164.2
	^{230}Th		
0.0	0.0	308.5	100.0[b]
635.1(2)	634.9(1)	117.3	31.9
1297.8(6)		6.7	1.5
1447.9(5)		2.6	0.6
1590.2(5)	1589.8(3)	16.2	3.4
1639.3(6)	1638.5(2)[d]	9.6	2.0
1802.5(6)		3.3	0.7
2093.9(7)		15.2	2.8
2150.5(6)		16.3	3.0
2175.1(6)		29.5	5.4
2268.9(6)		35.5	6.4
2395.2(7)		5.4	0.9
2493.8(7)		4.0	0.7
2528.1(7)		29.1	4.9
Σ			164.2
	^{232}U		
0.0	0.0	235.5	100.0[b]
691.4(3)	691.21(24)	71.4	26.0
1277.2(4)		17.5	5.7
1482.0(4)		22.5	7.1
1569.0(4)		5.4	1.7
1797.0(4)		12.3	3.7
1822.1(4)		32.9	9.8
1861.5(4)		15.7	4.6
1931.8(4)		44.6	13.0
Σ			171.6

[a]The relative errors of the cross sections result from counting statistics and background subtraction; they vary between 2% for strong states and 10% for weak states.
[b]By definition, see text.
[c]From Ref. [28].
[d]Assigned as $(2,0^+)$ in Ref. [34].

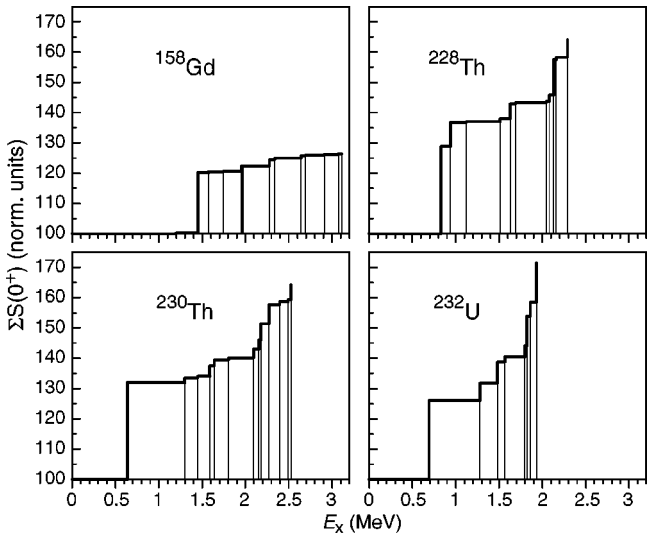

FIG. 11. Incremental plot of the transfer strengths to excited 0^+ states in ^{158}Gd, ^{228}Th, ^{230}Th, and ^{232}U. The ^{158}Gd data are derived from Ref. [30].

tions, which for different orbits differ in magnitude and—for cases with small cross sections—to some extent also in shape. Since small cross sections may be altered due to inelastic scattering (coupled channel effects) these deviations without further theoretical guidance are not considered as a basis to differentiate in the excitation of states between collective and noncollective excitations.

To determine spectroscopic factors we need a form factor as reference. Since in the present state of analysis we do not know the relative contributions of the specific j^2 transfer configurations to each of the observed excited 0^+ states—according to their microscopic structure—we arbitrarily chose one configuration which provides the best reproduction of the ground state transition, which is the $(2g_{9/2})^2$ transfer, as a reference. For each state the binding energies of the two neutrons are calculated to match the outgoing triton energy observed in (p,t). We used the code CHUCK3 of Kunz [60]. In this way we obtain a kinematic correction of the cross section, not more. With this restriction the term spectroscopic factor is used.

In Fig. 9 DWBA cross section angular distributions are compared with data for the observed transfers to the ground states of ^{228}Th, ^{230}Th, and ^{232}U. Their obtained spectroscopic factors, i.e., $(d\sigma/d\Omega)^{\mathrm{expt}}/(d\sigma/d\Omega)^{\mathrm{CHUCK3}}$, of 7.7, 8.7, and 8.0, respectively, are nearly the same, in agreement with earlier observations. Anyhow, the values depend strongly on the chosen potential parameters. We used the optical potential parameters listed in Table I; the resulting CHUCK3 input files are displayed in Fig. 15 in the Appendix.

To determine the spectroscopic factors of the excited states, we compare the experimental values of the differential cross section at the detection angle $\theta=7.5°$ with the DWBA-calculated value at the respective kinematic condition. The energy dependences of the ratios of the DWBA-calculated cross sections of excited states to the ground state cross sections are shown in Fig. 10. In this way the spectroscopic factors are determined as a kinematic correction of the cross

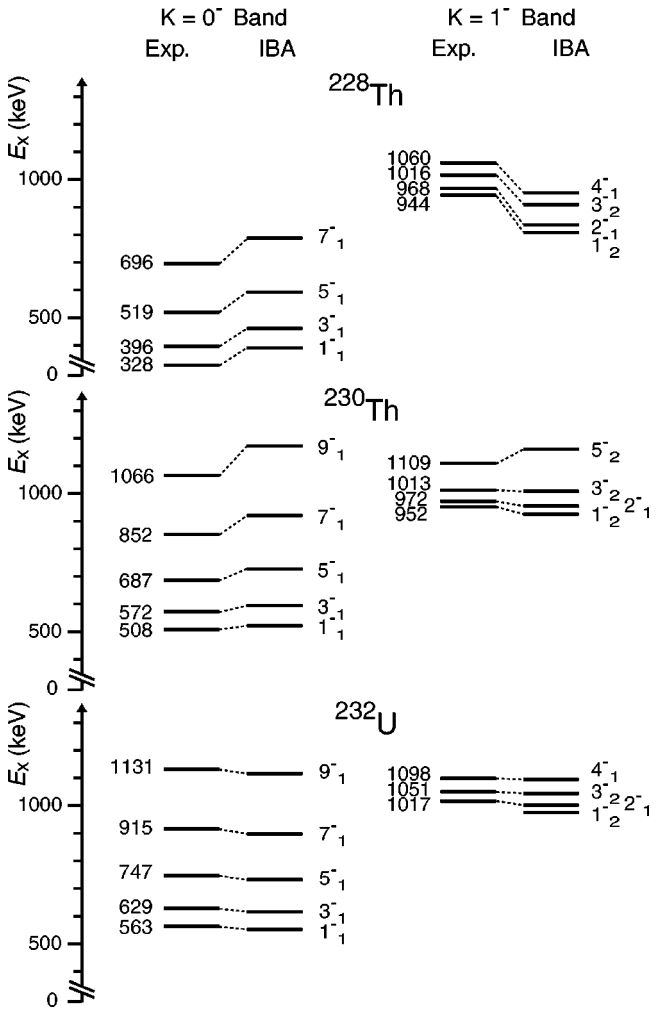

FIG. 12. Lowest negative parity bands in ^{228}Th, ^{230}Th, and ^{232}U, comparing the *spdf*-IBA calculation with known excitation energies from the NDS [33–35] and Ref. [28]. Left side experimental, right side calculated levels.

section. Since we do not attempt to fit the angular distributions of excited states, we show the data in Figs. 5–7 only with lines guiding the eye.

The results are summarized in Table II and in Fig. 11, where the spectroscopic factors are normalized to the respective observed ground state transfer strength, and given in percent of the latter. In Fig. 11 we display the transfer strength of all excited 0^+ states observed in ^{228}Th, ^{230}Th, and ^{232}U. We also include the data for ^{158}Gd from Ref. [30] to present all existing data for deformed nuclei, studied in a comparable way. The display as incremental plots visualizes the distribution of the transfer strength.

There are a few transitions with very low cross sections in the 1 μb/sr range which show for very small scattering angles an increasing cross section with decreasing angle, but otherwise not the typical pattern for a 0^+ excitation. We leave the discussion of these states to a forthcoming paper [31] and discuss here only states where the data provide firm evidence for 0^+ excitations. In the range of low cross sections, higher order and coupled channel effects may produce angular distributions which deviate strongly from those for one-step di-

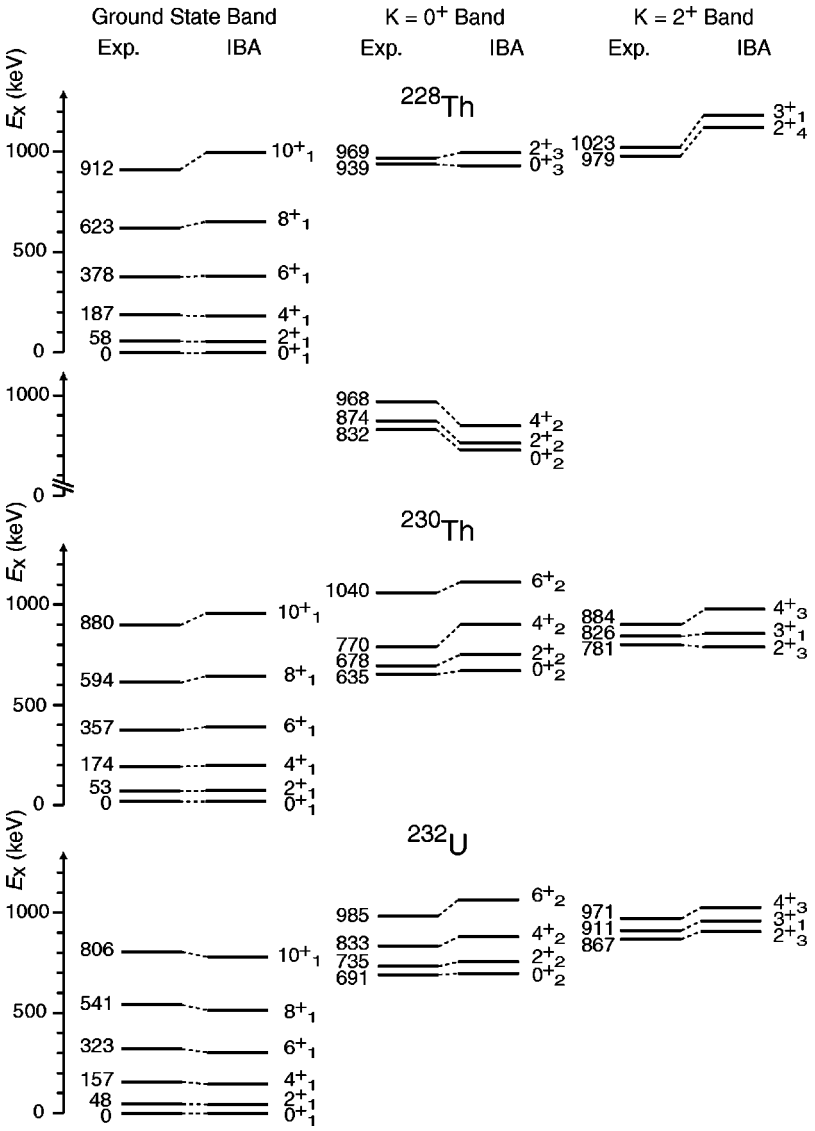

FIG. 13. Lowest positive parity bands in ^{228}Th, ^{230}Th, and ^{232}U, comparing the *spdf*-IBA calculation with known excitation energies from the Nuclear Data Sheets (NDS) [33–35] and Ref. [28]. For ^{228}Th we show two 0^+ bands. According to the schematic IBA calculation the octupole two-phonon band is the one with the lower excitation energies. In reality the two bands are expected to mix.

rect excitations. Thus we cannot claim to observe all excited 0^+ states. Our analysis is restricted to those showing up with a spectroscopic strength of about 0.5% of the ground state excitation strength or more, defining in this way a class of states.

In Fig. 11 we include also data for ^{158}Gd, derived from the cross sections of Lesher *et al.* [30]. Because of weak excitation strength, the first excited 0^+ state in ^{158}Gd at $E_x = 1195$ keV is not visible in this plot. For ^{228}Th, ^{230}Th, and ^{232}U, which differ by one neutron or one proton pair only, the summed 0^+ transfer strengths to the excited states add up to 64, 64, and 72 %, respectively, of the ground state transfer strengths. These are much higher values than observed for ^{158}Gd, where the excited states carry only 26% of the ground state transfer strength. Note the identical values for the two Th isotopes, and the larger value for ^{232}U with one additional proton pair.

TABLE III. Multipole parameters of the *spdf* boson IBA calculation. The number of negative parity bosons is allowed to range from 0 to 3.

Nucleus	^{232}U	^{230}Th	^{228}Th
Total number of bosons	12	11	10
ϵ_s	0.0000	0.0000	0.0000
ϵ_p	0.9900	1.0000	1.0500
ϵ_d	0.2500	0.2500	0.2100
ϵ_f	0.9400	0.9000	0.6500
κ	0.0120	0.0140	0.0180
χ_{sd}	1.3228	1.0000	1.3228

IV. COMPARISON OF 0^+ STATES WITH IBA CALCULATIONS

The role of the octupole degree of freedom in heavy deformed nuclei and the related description with *f* bosons, added to the established IBA in the *sd* boson space (*sd*-IBA), has been systematically studied for deformed rare earth nuclei [47] and for deformed actinides [48].

For the rare earth nuclei the IBA in the *sdf* boson space (*sdf*-IBA) reproduces reasonably well the main features of

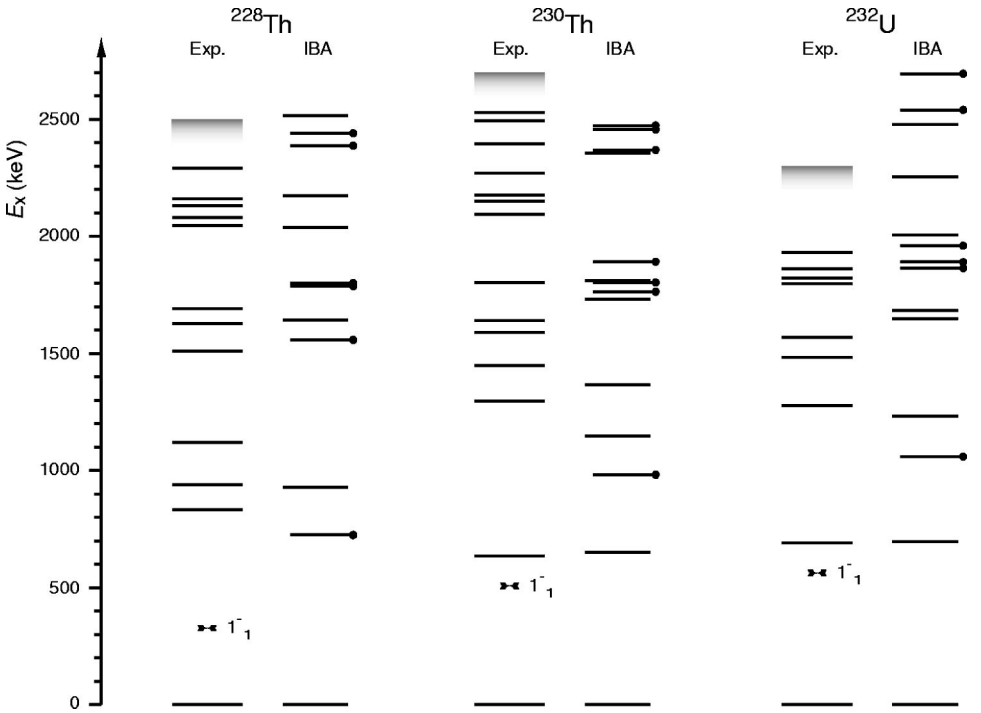

FIG. 14. Excitation energies of all safely assigned excited 0^+ states in ^{228}Th, ^{230}Th, and ^{232}U, compared with *spdf*-IBA calculations. OTP states are marked by a dot. The shadowed areas indicate the upper range of the experimental evaluation. The positions of the 1^-_1 states are indicated, too.

the observed low-lying negative parity states, for the actinide nuclei a better reproduction of the respective data is obtained if one allows in addition to the *f* boson for a *p* boson (*spdf*-IBA). The physical nature of the *p* boson is not clear. It may result as an artefact, or an anharmonicity, of an octupole excitation in a quadrupolar deformed potential. In the present context we treat the *f* boson or the combination of a *p* and an *f* boson (*pf* boson) as a technical way to describe octupole collectivity.

A simple IBA Hamiltonian in the *spdf* space, including vibrational contributions and a quadrupole interaction in the simple form, is

$$H = \epsilon_d \hat{n}_d + \epsilon_p \hat{n}_p + \epsilon_f \hat{n}_f - \kappa \hat{Q}_{spdf} \cdot \hat{Q}_{spdf}, \tag{1}$$

where ϵ_d, ϵ_p, and ϵ_f are the boson energies and $\hat{n}_d$, $\hat{n}_p$, and $\hat{n}_f$ are the boson number operators. Note that the same strength κ of the quadrupole interaction describes the *sd* bosons and the *pf* bosons. The $\hat{Q}_{spdf}$ quadrupole operator

$$\begin{aligned}\hat{Q}_{spdf} = \hat{Q}_{sd} + \hat{Q}_{pf} = [s^\dagger \tilde{d} + d^\dagger s]^{(2)} - (1/2)\sqrt{7}[d^\dagger \tilde{d}]^{(2)} \\ + (3/5)\sqrt{7}[p^\dagger \tilde{f} + f^\dagger \tilde{p}]^{(2)} - (9/10)\sqrt{3}[p^\dagger \tilde{p}]^{(2)} \\ - (3/10)\sqrt{42}[f^\dagger \tilde{f}]^{(2)}\end{aligned} \tag{2}$$

is used as in Ref. [51]; the $-\sqrt{7}/2$ factor in front of $[d^\dagger \tilde{d}]^{(2)}$ may be adjusted introducing an additional parameter χ_{sd}. This Hamiltonian was used in Refs. [32,51].

In Figs. 12 and 13 we display excitation energies of negative and positive parity states in ^{228}Th, ^{230}Th, and ^{232}U, comparing an *spdf*-IBA calculation with experimental data from the Nuclear Data compilations [33–35]. The *pf* boson parameters are chosen to reproduce the $K^\pi = 0^-$ and $K^\pi = 1^-$ bandheads; they are determined by the experimental energies of the $J^\pi = 1^-_1, K^\pi = 0^-$ and $J^\pi = 1^-_2, K^\pi = 1^-$ states. For ^{228}Th the $J^\pi = 1^-_1, K^\pi = 0^-$ excitation energy is 328 keV and thus significantly lower than 508 and 563 keV for ^{230}Th and ^{232}U, respectively. This is in contrast to the $J^\pi = 1^-_2, K^\pi = 1^-$ excitation energies, which are about the same in the three nuclei, compare Fig. 12.

The IBA parameters in the *sd* boson space are determined by the low energy spacing of the ground state band and the $J^\pi = 2^+_1, K^\pi = 0^+$ and $J^\pi = 2^+_1, K^\pi = 2^+$ bandheads, respectively. The values of the parameters are listed in Table III.

The experimental spectra of the 0^+ states obtained for ^{228}Th, ^{230}Th, and ^{232}U, and the results of *spdf*-IBA calculations are compared in Fig. 14; as for ^{158}Gd [32], in the *spdf*-IBA calculations mixing between *d* and *pf* bosons is neglected and the *f* (and *p*) bosons account for octupole collectivity. The key quantities for octupole collectivity, the 1^- excitation energies, are also indicated.

For ^{228}Th, ^{230}Th, and ^{232}U in the energy ranges covered experimentally (2.5, 2.7, and 2.3 MeV, respectively) the IBA predicts four, six, and six excited 0^+ states, respectively, of pure *sd* (quadrupolar) bosonic structure, and additionally six, seven, and four excited 0^+ states, respectively, which have two bosons in the *pf* boson space. They are related to—or represent—OTP excitations. Inspecting the lowest excited 0^+ states of ^{228}Th, ^{230}Th, and ^{232}U we have a reasonable correlation in excitation energy between experiment and calculation.

For all of these three nuclei this schematic calculation predicts one of the two lowest excited 0^+ states as an octupole two-phonon excitation and the other one as an *sd* space excitation; the sequence, however, changes. Because of the larger octupole collectivity of ^{228}Th, expressed by the low value of the excitation energy of the lowest 1^- state at 328 keV, the predicted octupole two-phonon 0^+ excitation is lower in excitation energy than the predicted lowest excited

```
1009000030000000     230Th(p,t)228Th Ex=0.0 MeV 2g9/2
+150.    +01.    +0.5
+40+02+00+00
+00.1   +20.
+25.0   +01.0078+01.    +230.00 +90.    +01.30          +00.85  +01.
+01+01
+01.    -57.10  +1.1700 +0.750          -02.80  +1.320  +00.510
+02.                                   +32.46  +1.320  +00.510
-04.    -24.8   +01.01  +00.75
-03.567 +03.016 +01.    +228.00 +90.    +01.30          +00.25  +01.    -0.000
+02+02
-01.    -166.70 +1.1600 +0.752          -10.28  +1.498  +00.817
-02-01+00+00+00+02+00+00-1560.00                        +00.00
+01.    +05.    +00.    +01.00
-06.016 +01.008 +00.    +228.00 +90.                                   +0.000
-01.    -01.    +01.17  +00.75  +25.
+01.    +04.    +09.    +01.    +60.
+00
+00+00
9                       END OF CHUCK3 INPUT

1009000030000000     232Th(p,t)230Th Ex=1.5 MeV 2g9/2
+150.    +01.    +0.5
+40+02+00+00
+00.1   +20.
+25.0   +01.0078+01.    +232.00 +90.    +01.30          +00.85  +01.
+01+01
+01.    -57.10  +1.1700 +0.750          -02.80  +1.320  +00.510
+02.                                   +32.46  +1.320  +00.510
-04.    -24.8   +01.01  +00.75
-03.075 +03.016 +01.    +230.00 +90.    +01.30          +00.25  +01.    -1.500
+02+02
-01.    -166.70 +1.1600 +0.752          -10.28  +1.498  +00.817
-02-01+00+00+00+02+00+00-1560.00                        +00.00
+01.    +05.    +00.    +01.00
-05.779 +01.008 +00.    +230.00 +90.                                   +0.750
-01.    -01.    +01.17  +00.75  +25.
+01.    +04.    +09.    +01.    +60.
+00
+00+00
9                       END OF CHUCK3 INPUT

1009000030000000     234U(p,t)232U Ex=3.0 MeV 2g9/2
+150.    +01.    +0.5
+40+02+00+00
+00.1   +20.
+25.0   +01.0078+01.    +234.00 +92.    +01.30          +00.85  +01.
+01+01
+01.    -57.10  +1.1700 +0.750          -02.80  +1.320  +00.510
+02.                                   +32.46  +1.320  +00.510
-04.    -24.8   +01.01  +00.75
-04.122 +03.016 +01.    +232.00 +92.    +01.30          +00.25  +01.    -3.000
+02+02
-01.    -166.70 +1.1600 +0.752          -10.28  +1.498  +00.817
-02-01+00+00+00+02+00+00-1560.00                        +00.00
+01.    +05.            +01.00
-06.294 +01.008 +00.    +232.00 +92.                                   +1.500
-01.    -01.    +01.17  +00.75  +25.
+01.    +04.    +09.    +01.    +60.
+00
+00+00
9                       END OF CHUCK3 INPUT

1009000030000000     160Gd(p,t)158Gd Ex=0.5 MeV 1h9/2
+150.    +01.    +0.5
+40+02+00+00
+00.1   +20.
+27.0   +01.0078+01.    +160.00 +64.    +01.25          +00.85  +01.
+01+01
+01.    -58.88  +1.230  +0.750          -03.24  +1.320  +00.650
+02.                                   +29.80  +1.320  +00.650
-04.    -24.8   +01.01  +00.75
-04.913 +03.016 +01.    +158.00 +64.    +01.30          +00.25  +01.    -0.500
+02+02
-01.    -160.03 +1.200  +0.720          -17.83  +1.400  +00.840
-02-01+00+00+00+02+00+00-1560.00                        +00.00
+01.    +05.            +01.00
-06.697 +01.008 +00.    +158.00 +64.                                   +0.250
-01.    -01.    +01.17  +00.75  +25.
+00.    +05.    +09.    +01.    +60.
+00
+00+00
9                       END OF CHUCK3 INPUT
```

FIG. 15. CHUCK3 input files for the discussed (p,t) reactions.

0^+ states in the *sd* space. The situation is reversed for ^{230}Th and ^{232}U, where the lowest 1^- states have higher excitation energies, compare Fig. 14.

Taking the IBA calculation and the parametrization used literally, the IBA predicts in the energy ranges considered 10, 13, and 10 excited 0^+ states. Accounting in addition for the presence of a monopole pairing vibrational state, and perhaps one state from hexadecupole collectivity, both not included in the calculation, we have—without consideration of non collective two-quasiparticle states—nearly perfect agreement with the numbers of 11, 13, and 8 observed and safely assigned states for ^{228}Th, ^{230}Th, and ^{232}U, respectively.

To improve the comparison with theory one needs information about the spectroscopic factors. The IBA, in lowest order, fails completely to reproduce the (p,t) spectroscopic factors. The calculated first excited 0^+ state comes with about 1% of the transfer strength of the ground state, and the higher states are even weaker, whereas experimentally the excited states show up with about 60% of the ground state transfer strength. The IBA as well as most RPA calculations do not include the monopole pairing vibrational configurations. The spreading of this strength, however, is the mechanism which provides the (p,t) transfer.

V. CONCLUSION

We have performed (p,t) transfer reactions to study excited 0^+ states in ^{228}Th, ^{230}Th, and ^{232}U. In each of these three nuclei we find several excited 0^+ states that have not been experimentally observed before. Their accumulated strengths add up to more than 60% of the ground state strengths.

An *spdf*-IBA description of these actinide nuclei gives a nearly quantitative prediction of the number of the observed excited 0^+ states. This interesting, but puzzling result and the large observed transfer strengths need microscopic explanations. We hope data of this kind will stimulate further and microscopically motivated studies, as those in the QPM model [25–28] or in BCS and RPA models as in Ref. [19], but in a large configuration space. In this respect it will be interesting to see whether the very large observed accumulated strengths of the excited states of more than 60% of the ground state strengths result from a kind of splitting of the ground state strengths, due to quadrupole pairing in combination with a nonstatistical distribution of prolate and oblate orbitals, as discussed above. If the transfer strengths to the first excited states have to be considered as part of the ground state strength, then the remaining strengths of the higher excited states stay in the 25% range, as observed for ^{158}Gd, compare Fig. 11.

ACKNOWLEDGMENTS

The authors appreciate stimulating discussions with P. von Brentano, R. Broglia, R. F. Casten, V. Yu. Ponomarev, and P. Ring. We thank H. J. Maier for preparation of the targets. The work was supported by the DFG (Grant Nos. C4-Gr894/2-3, Gu179/3, and Jo391/2-1), MLL, U.S.-DOE, Contract No. DE-FG02-91ER-40609, and by the European Community program IHP, Contract No. HPMF-CT-2002-02018.

APPENDIX: DWBA INPUT FILES

Figure 15 shows the four input files used for the DWBA calculations with the code CHUCK3. The optical potential parameters are given in Table I.

[1] R. Julin, J. Kantele, J. Kumpulainen, M. Luontama, A. Passoja, W. Trzaska, E. Verho, and J. Blomqvist, Phys. Rev. C **36**, 1129 (1987).
[2] M. Yeh, P. E. Garrett, C. A. McGrath, S. W. Yates, and T. Belgya, Phys. Rev. Lett. **76**, 1208 (1996).
[3] S. W. Yates, M. Yeh, M. Kadi, C. A. McGrath, P. E. Garrett, and T. Belgya, J. Phys. G **25**, 691 (1999).
[4] B. D. Valnion, V. Yu. Ponomarev, Y. Eisermann, A. Gollwitzer, R. Hertenberger, A. Metz, P. Schiemenz, and G. Graw, Phys. Rev. C **63**, 024318 (2001).
[5] S. A. Fayans, A. P. Platonov, G. Graw, and D. Hofer, Nucl. Phys. **A577**, 557 (1994).
[6] R. Hertenberger, G. Eckle, F. J. Eckle, G. Graw, D. Hofer, H. Kader, P. Schiemenz, Gh. Cata-Danil, C. Hategan, N. Fujiwara, K. Hosono, M. Kondo, N. Matsuoka, T. Noro, T. Saito, S. Kato, S. Matsuki, N. Blasi, S. Micheletti, and R. De Leo, Nucl. Phys. **A574**, 414 (1994).
[7] V. Yu. Ponomarev, M. Pignanelli, N. Blasi, A. Bontempi, J. A. Bordewijk, R. De Leo, G. Graw, M. N. Harakeh, D. Hofer, M. A. Hofstee, S. Micheletti, R. Perrino, and S. Y. van der Werf, Nucl. Phys. **A601**, 1 (1996).
[8] A. M. Oros, P. von Brentano, R. V. Jolos, L. Trache, G. Graw, G. Cata-Danil, B. D. Valnion, A. Gollwitzer, and K. Heyde, Nucl. Phys. **A613**, 209 (1997).
[9] Gh. Cata-Danil, D. Bucurescu, L. Trache, A. M. Oros, M. Jaskola, A. Gollwitzer, D. Hofer, S. Deylitz, B. D. Valnion, and G. Graw, Phys. Rev. C **54**, 2059 (1996).
[10] M. Jaskola, P. Guazzoni, L. Zetta, A. Covello, A. Gargano, Y. Eisermann, G. Graw, and R. Hertenberger, Acta Phys. Pol. B **33**, 363 (2002).
[11] A. I. Levon, J. de Boer, G. Graw, R. Hertenberger, D. Hofer, J. Kvasil, A. Lösch, E. Müller-Zanotti, M. Würkner, H. Baltzer, V. Grafen, and C. Günther, Nucl. Phys. **A576**, 267 (1994).
[12] L. Trache, A. M. Oros, Gh. Cata-Danil, K. O. Zell, P. von Brentano, G. Graw, D. Hofer, and E. Müller-Zanotti, Phys. Rev. C **49**, R1742 (1994).
[13] M. A. Oothoudt and N. M. Hintz, Nucl. Phys. **A213**, 221 (1973).
[14] J. V. Maher, J. R. Erskine, A. M. Friedman, R. H. Siemssen, and J. P. Schiffer, Phys. Rev. Lett. **52**, 302 (1970); Phys. Rev. C **5**, 1380 (1972).
[15] R. E. Griffin, A. D. Jackson, and A. B. Volkov, Phys. Lett. **36B**, 281 (1971).
[16] W. I. van Rij and S. H. Kahana, Phys. Rev. Lett. **28**, 50 (1972).
[17] D. R. Bess, R. A. Broglia, and B. Nilsson, Phys. Lett. **40B**, 338 (1972).
[18] R. F. Casten, E. R. Flynn, J. D. Garrett, O. Hansen, T. J. Mulligan, D. R. Bess, R. A. Broglia, and B. Nilsson, Phys. Lett. **40B**, 333 (1972).
[19] I. Ragnarsson and R. A. Broglia, Nucl. Phys. **A263**, 315 (1976).
[20] M. H. Mortensen, R. R. Betts, and C. K. Bockelmann, Phys. Rev. C **21**, 2275 (1980).
[21] B. Ackermann, H. Baltzer, K. Freitag, C. Günther, P. Herzog, J. Manns, U. Müller, R. Paulsen, P. Sevenich, T. Weber, B. Will, J. de Boer, G. Graw, A. I. Levon, M. Loewe, A. Lösch, and E. Müller-Zanotti, Z. Phys. A **350**, 13 (1994).
[22] H. Baltzer, K. Freitag, C. Günther, P. Herzog, J. Manns, U. Müller, R. Paulsen, P. Sevenich, T. Weber, and B. Will, Z. Phys. A **352**, 47 (1995).
[23] H. Baltzer, J. de Boer, A. Gollwitzer, G. Graw, C. Günther, A. I. Levon, M. Loewe, H. J. Maier, J. Manns, U. Müller, B. D. Valnion, T. Weber, and M. Würkner, Z. Phys. A **356**, 13 (1996).
[24] T. Weber, J. de Boer, K. Freitag, J. Gröger, C. Günther, J. Manns, and U. Müller, Z. Phys. A **358**, 281 (1997).
[25] V. G. Soloviev, Z. Phys. A **334**, 143 (1989).
[26] N. Yu. Shirikova (private communication).
[27] V. G. Soloviev, A. V. Sushkov, and N. Yu. Shirikova, Nucl. Phys. **A568**, 244 (1994); Phys. Part. Nucl. **27**, 667 (1996); Prog. Part. Nucl. Phys. **38**, 53 (1997).
[28] T. Weber, J. de Boer, K. Freitag, J. Gröger, C. Günther, P. Herzog, V. G. Soloviev, A. V. Sushkov, and N. Yu. Shirikova, Eur. Phys. J. A **3**, 25 (1998).
[29] T. Otsuka and M. Sugita, J. Phys. Soc. Jpn. **58**, 530 (1989).
[30] S. R. Lesher, A. Aprahamian, L. Trache, A. Oros-Peusquens, S. Deyliz, A. Gollwitzer, R. Hertenberger, B. D. Valnion, and G. Graw, Phys. Rev. C **66**, 051305 (2002).
[31] A. I. Levon *et al.* (unpublished).
[32] N. V. Zamfir, J.-Y. Zhang, and R. F. Casten, Phys. Rev. C **66**, 057303 (2002).
[33] A. Artna-Cohen, Nucl. Data Sheets **80**, 723 (1997).
[34] Y. A. Akovali, Nucl. Data Sheets **69**, 155 (1993).
[35] M. R. Schmorak, Nucl. Data Sheets **63**, 139 (1991).
[36] N. Amzal, J. F.C. Cocks, P. A. Butler, K. J. Cann, P. T. Greenlees, G. D. Jones, S. Asztalos, R. M. Clark, M. A. Deleplanque, R. M. Diamond, P. Fallon, I. Y. Lee, A. O. Machiavelli, R. W. MacLeod, F. S. Stephens, P. M. Jones, R. Julin, R. Broda, B. Fornal, J. F. Smith, T. Lauritsen, P. Bhattacharyya, and C. T. Zhang, J. Phys. G **25**, 831 (1999).
[37] J. F.C. Cocks, D. Hawcroft, N. Amzal, P. A. Butler, K. J. Cann, P. T. Greenlees, G. D. Jones, S. Asztalos, R. M. Clark, M. A. Deleplanque, R. M. Diamond, P. Fallon, I. Y. Lee, A. O. Macchiavelli, R. W. MacLeod, F. S. Stephens, P. Jones, R. Julin, R. Broda, B. Fornal, J. F. Smith, T. Lauritsen, P. Bhattacharyya, and C. T. Zhang, Nucl. Phys. **A645**, 61 (1999).
[38] P. A. Butler and W. Nazarewicz, Rev. Mod. Phys. **68**, 349 (1996).
[39] A. A. Raduta, N. Lo Iudice, and I. I. Ursu, Nucl. Phys. **608**, 11 (1996); Nuovo Cimento Soc. Ital. Fis., A **109A**, 1669 (1996).
[40] R. V. Jolos and Yu. V. Palchikov, Yad. Fiz. **60**, 1202 (1997); Phys. At. Nucl. **60**, 1077 (1997).
[41] N. Minkov, S. B. Drenska, P. P. Raychev, R. P. Roussev, and D. Bonatsos, Phys. Rev. C **61**, 064301 (2000).
[42] A. R. Safarov, R. Kh. Safarov, and A. S. Sitdikov, Yad. Fiz. **64**, 1496 (2001); Phys. At. Nucl. **64**, 1419 (2001).
[43] A. Tsvetkov, J. Kvasil, and R. G. Nazmitdinov, J. Phys. G **28**, 2187 (2002).
[44] A. A. Raduta and D. Ionescu, Phys. Rev. C **67**, 044312 (2003).
[45] C. Y. Wu and D. Cline, Phys. Rev. C **54**, 2356 (1996).
[46] U. Meyer, A. A. Raduta, and A. Faessler, Nucl. Phys. **A641**, 321 (1998).
[47] P. D. Cottle and N. V. Zamfir, Phys. Rev. C **54**, 176 (1996).
[48] P. D. Cottle and N. V. Zamfir, Phys. Rev. C **58**, 1500 (1998).
[49] N. Minkov, S. B. Drenska, P. P. Raychev, R. P. Roussev, and D. Bonatsos, Phys. Rev. C **60**, 034305 (1999).
[50] A. F. Diallo, B. R. Barrett, P. Navratil, and C. Gorrichategui, Ann. Phys. (N.Y.) **279**, 81 (2000).
[51] N. V. Zamfir and D. Kusnezov, Phys. Rev. C **63**, 054306 (2001); **67**, 014305 (2003).

[52] S. C. Li and S. Kuyucak, Nucl. Phys. **A604**, 305 (1996).
[53] P. E. Garrett, H. Lehmann, J. Jolie, C. A. McGrath, M. Yeh, and S. W. Yates, in *Proceedings of the Conference on Capture Gamma-Ray Spectroscopy, Prague, 2002*, edited by J. Kvasil, P. Cejnar, and M. Krticka (World Scientific, Singapore 2003), p. 157
[54] M. Löffler, H. J. Scheerer, and H. Vonach, Nucl. Instrum. Methods **111**, 1 (1973).
[55] E. Zanotti, M. Bisenberger, R. Hertenberger, H. Kader, and G. Graw, Nucl. Instrum. Methods Phys. Res. A **310**, 706 (1991).
[56] H.-F. Wirth, H. Angerer, T. von Egidy, Y. Eisermann, G. Graw, and R. Hertenberger, Beschleunigerlaboratium München Annual Report, 2000, p. 71.
[57] H.-F. Wirth, Ph.D. thesis, Techn. Univ. München, 2001, see http://tumb1.biblio.tu-muenchen.de/publ/diss/ph/2001/wirth.html
[58] F. Rieß, Beschleunigerlaboratorium München Annual Report, 1991, p. 168.
[59] G. Ardisson, M. Hussonnois, J. F. LeDu, D. Trubert, and C. M. Lederer, Phys. Rev. C **49**, 2963 (1994).
[60] P. D. Kunz, computer code CHUCK3, University of Colorado, unpublished.
[61] C. M. Perey and F. G. Perey, At. Data Nucl. Data Tables **17**, 1 (1976).